Self-Reconfiguring Modular Robotic Boats

Wei Wang

wwang745@wisc.edu

University of Wisconsin-Madison https://orcid.org/0000-0003-4023-2845

Niklas Hagemann

Massachusetts Institute of Technology

Alejandro Gonzalez-Garcia

KU Leuven

Carlo Ratti

Massachusetts Institute of Technology

Daniela Rus

MIT https://orcid.org/0000-0001-5473-3566

Article

Keywords:

Posted Date: July 3rd, 2025

DOI: https://doi.org/10.21203/rs.3.rs-6942560/v1

Additional Declarations: There is **NO** Competing Interest.

Self-Reconfiguring Modular Robotic Boats

Wei Wang[1,†,*], Niklas Hagemann[2,*], Alejandro Gonzalez-Garcia[3,*], Carlo Ratti[4,5], Daniela Rus[2,†]

[1]*Marine Robotics Lab, Department of Mechanical Engineering, College of Engineering, University of Wisconsin-Madison, Madison, USA*

[2]*Computer Science and Artificial Intelligence Lab (CSAIL), Massachusetts Institute of Technology, Cambridge, USA*

[3]*MECO Research Team, Department of Mechanical Engineering, KU Leuven, Belgium*

[4]*Senseable City Laboratory, Massachusetts Institute of Technology, Cambridge, USA*

[5]*ABC Department, Politecnico di Milano, Milano, Italia*

[*]These authors contributed equally to this work.

ABSTRACT

Self-reconfigurable aquatic robots offer promising potential for a wide range of marine applications, including building temporary infrastructure, environmental monitoring, and on-demand transportation. However, achieving autonomous water-based self-reconfiguration, even in two dimensions on the water surface, remains challenging, due to complex nonlinear hydrodynamics, disturbances from self-motion and neighboring robots, as well as external environmental factors. Here, we present the *FloatForm* platform, a group of miniature modular robotic boats, capable of self-assembling into physically connected structures, self-reconfiguring, and collectively traveling as larger assemblies via a hybrid coordination framework. Each robot unit is equipped with onboard sensing, motion control, and the ability to coordinate and physically latch with its neighbors. We demonstrate the feasibility of parallel self-reconfiguration, where distributed controllers on each robot handle coordination tasks such as aggregating into desired shapes and avoiding collisions, while a minimalist central planner oversees the overall success of each task and fixes imperfections. This work advances the design, control, and coordination of modular robotic systems in aquatic environments, paving the way for flexible, robust and scalable applications on the water.

INTRODUCTION

Modular self-reconfigurable robot (MSRR) systems[1-17] consist of multiple robot modules that can connect and collaborate to form larger, adaptable robotic structures. A key feature of these systems is their ability to self-reconfigure, allowing modules to rearrange their connections to create structures optimized for specific tasks and environments[18,19]. As the number of robots in an MSRR system increases, the complexity of their interactions also grows. However, this complexity enables the systems to exhibit greater versatility and robustness, allowing them to perform a wide range of tasks and effectively manage failures of individual modules.

Recent advances have demonstrated a variety of successful implementations of MSRR systems[18,20-29], both on the ground and in the air. The Kilobot project demonstrated large-scale two-dimensional (2D) shape self-assembly[20], using a distributed algorithm that leverages simple capabilities such as edge-following, gradient formation, and localization. Roombots[21-23] demonstrated modular furniture that moves, self-assembles, and self-reconfigures in 3D. The M-block project[24,25] introduced a novel hardware system that uses pulses of angular momentum and magnetic hinges to move modules and self-assemble 3D structures. In the air, a group of flying robots, ModQuads, illustrated self-assembly and collective flight[27], while the terrestrial SMORES-EP modular robots[18] have shown the ability to complete high-level tasks by dynamically reconfiguring to adapt to previously unknown environments.

By contrast, aquatic MSRR systems remain in their infancy despite offering unique potential for ocean exploration, adaptive transportation, and dynamic marine infrastructure[30-34]. Such systems could form on-demand floating platforms to support offshore operations, ranging from environmental response to adaptive infrastructure (Fig. 1g -1h), and later disassemble or self-reconfigure to minimize ecological footprint and enhance logistical efficiency. Analogous behaviors are observed in nature: red fire ants dynamically self-assemble into floating rafts to survive seasonal flooding[35,36]. Emulating this strategy, aquatic MSRR systems could autonomously form stable, cohesive structures to endure extreme maritime conditions. However,

deploying MSRR systems in aquatic environments introduces a distinct set of challenges. Self-reconfiguration in open water requires real-time control over complex, nonlinear hydrodynamics, compounded by persistent disturbances from self-induced motion, inter-module interactions, and external forces such as waves, currents, and wind. These dynamic conditions can frequently disrupt control, coordination, and alignment, demanding robust control architectures and fault-tolerant docking mechanisms. Overcoming these challenges is essential to unlock the full potential of modular robotic systems in aquatic domains.

Several modular self-reconfigurable robotic (MSRR) systems have explored self-assembly in aquatic environments, with early demonstrations highlighting the potential of robotic boats to autonomously form floating platforms. These systems typically employed centralized frameworks for sequencing, trajectory planning, and docking control, enabling coordinated behaviors such as sequential assembly or collective swimming in underactuated robot lattices. Notable examples include floating platform self-assembly using centralized planners[32,33,37] and the Modboat project, which demonstrated centralized control for group locomotion in a parallel lattice of aquatic modules[38]. Despite these advances, existing aquatic MSRR systems remain constrained by their reliance on fully centralized coordination. Such architectures are inherently vulnerable to single-point failures, particularly in dynamic and uncertain aquatic environments where individual module malfunctions or communication loss can cascade into system-wide deadlocks. Centralized control also scales poorly, with computational burdens increasing rapidly with the number of units—posing fundamental challenges for real-time responsiveness and robustness. Moreover, current systems lack the capability for parallel assembly, a critical requirement for achieving rapid and adaptive configuration in the face of environmental disturbances.

To overcome these limitations, we present ***FloatForm***, a novel aquatic MSRR platform operating under a hybrid control architecture that combines minimal centralization with predominantly distributed coordination. Each *FloatForm* module has onboard sensing, state estimation, control capabilities, and latching mechanisms that facilitate autonomous assembly and reconfiguration. The architecture incorporates a lightweight centralized planner for high-level tasks, such as correcting imperfect positions in shape formation,

while most coordination behaviors, including shape formation and collision avoidance, are governed by distributed controllers. State information is exchanged with neighboring units through intercommunication. Notably, self-assembly and self-reconfiguration are executed in a parallel and highly decentralized manner, allowing all robots to continuously coordinate and adjust their states collectively. This hybrid framework, which balances local autonomy with global oversight, markedly improves the scalability, robustness, and real-world applicability of aquatic MSRR systems.

RESULTS

Modular aquatic robot design with active latching and feedback control

We have designed and fabricated a group of eight *FloatForm* robot boats, each measuring L (0.21 m) × W (0.21 m) × H (0.14 m), as a platform for studying self-assembly and self-reconfiguration in the aquatic domain. Each robot is an autonomous floating robot with onboard sensing, control, and actuators, giving the ability to autonomously achieve a desired state in the presence of surrounding disturbances. A key feature of each robot is its capability to latch to other units. Latching is particularly challenging in aquatic settings due to the need for a broad working range to account for unpredictable disturbances. An overview of the system and its potential applications is presented in Fig. 1.

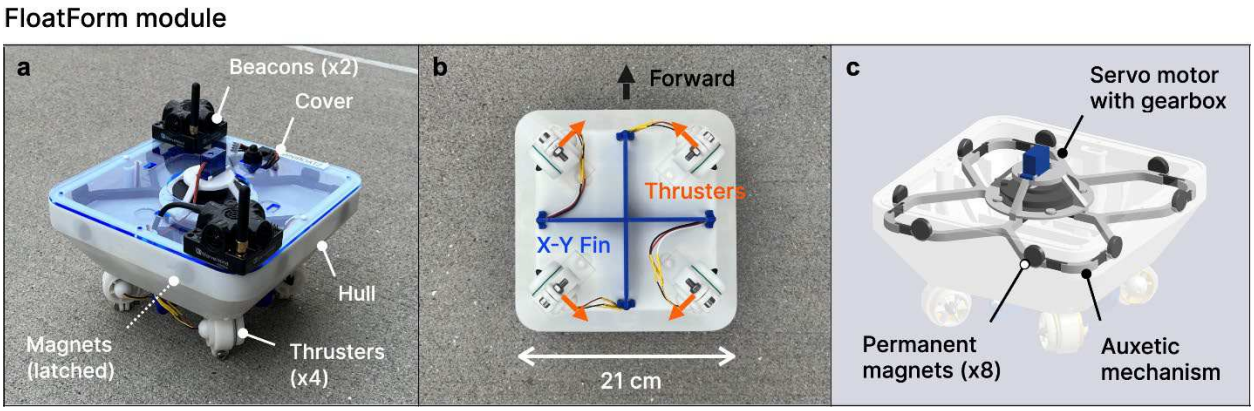

Fig. 1. Modular *FloatForm* platform. (**a**) An overview of a single *FloatForm* module, including a 3D-printed hull, customized miniature thrusters, ultrasonic beacons, Inertial Measurement Unit (IMU), and an enclosed magnetic latching system based around an origami-inspired mechanism. (**b**) Bottom view of a single robot, highlighting the thruster arrangement and stabilizing 'cross' fin, to increase rotational inertia. (**c**) The origami-inspired latching mechanism to actuate the permanent magnets. (**d**) Eight *FloatForm* modules after self-assembly, moving in formation. (**e**) Illustration of the experimental setup, featuring four fixed ultrasonic beacons positioned at the corners of the test pool (dimensions: 4.0 × 2.7 × 1.2 m); these fixed

beacons, analogous to GPS satellites, are elevated one meter above the water surface to ensure maximal coverage. (**f-h**) potential applications of self-assembling and reconfiguring robot boat swarms: monitoring and containing an environmental hazard; a search-and-rescue mission with boats searching independently and coming back together to form a raft; building adaptive, resilient infrastructure in remote areas while exposed to environmental disturbances like waves and currents.

The square footprint of the *FloatForm* robot (Fig. 1a), allows for flexible self-assembly into arbitrary square lattices. High maneuverability is critical for effective control and latching during coordination. To achieve this, four miniature thrusters are arranged in an "X" configuration (Fig. 1b, Supplementary Fig. 3), allowing for omnidirectional motion, including both longitudinal and lateral translation, as well as on-the-spot rotation (see Supplementary Video 1). Stability during dynamic maneuvers is enhanced by strategically positioning internal components (like the battery) to maintain a low center of gravity and aligning these with the center of buoyancy. To compensate for the inherently low rotational inertia of the robot, a set of stabilizing fins (visible in the bottom view, Fig. 1b) is incorporated along the x and y axes. These fins increase hydrodynamic drag, reducing rotational actuation sensitivity at near-zero speeds and improving control performance in aquatic environments.

To enable reliable self-assembly and self-reconfiguration on the water, each robot must be capable of mechanically latching with neighboring boats. To achieve this, a fully enclosed magnetic latching system was designed with the goal of reliably connecting with other boats even under disturbances. An origami-inspired mechanism allows a single servo motor located in the center of the robot to simultaneously actuate permanent magnets on all four sides of the robot (Fig 1c, Supplementary Fig. 1). Permanent magnets are arranged by alternating polarity, with two magnets per side (Supplementary Fig. 1 and Supplementary Fig. 2a), ensuring boats latch reliably across 10-12 cm gaps, without the added weight or sustained power draw of electromagnets. A custom 3D-printed gearbox is integrated, allowing the use of a simple lightweight

servo motor and adding sufficient mechanical inertia for the system to maintain either a latched or unlatched state without any power draw (Supplementary Fig. 1 and Supplementary Fig. 2, Supplementary Video 2).

The *FloatForm* robots utilize off-the-shelf acoustic beacons for self-localization. Fig. 1e shows four stationary ultrasonic beacons located at the corners of the test pool, providing fixed reference points (analogously to GPS satellites). Each robot is equipped with two mobile beacons, enabling precise inference of position and heading (see Fig. 1a and Supplementary Fig. 4). Localization is achieved by estimating the propagation delay of ultrasonic pulses relative to the stationary beacons (Time-Of-Flight), which is then processed using a trilateration algorithm. To enhance accuracy and provide high-frequency state estimation, a Kalman filter integrates the data from the beacons with inertial measurements from the onboard IMU, yielding a refined estimate of the robot's pose, velocity, and acceleration.

The design of low-level motion controllers for the *FloatForm* modules is driven by the unique challenges of aquatic environments, including nonlinear hydrodynamics and disturbances arising from self-motion or neighboring units. To address these challenges, each robot is equipped with a low-level feedback controller running on an embedded computer. The controller regulates the reference heading angle and ensures precise velocity control in surge and sway directions. The control architecture is based on a combination of Proportional-Integral-Derivative (PID) control and feedback linearization, effectively compensating for aspects of the robot's nonlinear dynamics and disturbances (see more details in Methods and Supplementary Note 2).

The *FloatForm* hardware is designed with a strong focus on modularity, robust latching, onboard sensing, and feedback control. A detailed overview of the hardware design and control strategies is provided in the Methods section and Supplementary Materials. In this study, we showcase the capabilities of the *FloatForm* system using a fleet of eight robotic units (Fig. 1d) that autonomously self-assemble and reconfigure into various two-dimensional structures within a controlled freshwater tank measuring 4.0 m × 2.7 m × 1.2 m (Fig. 1e). All two-dimensional trajectories are recorded for post-experimental analysis.

Self-reconfiguring Robotic Boats

Seen as a collective, the *FloatForm* system is designed with three fundamental capabilities: (i) self-assembly, facilitating the parallel formation of physically connected structures; (ii) self-reconfiguration, enabling the swarm to disassemble and reassemble into new physically connected configurations in parallel; and (iii) collective transport, allowing the assembled swarm to navigate as a cohesive unit across the water. Figure 2 provides an overview of the three collective capabilities of the aquatic 2D MSRR system. The self-assembly process unfolds through the sequence illustrated in Fig. 2a–f. Self-reconfiguration, illustrated in Fig. 2g and h, consists of self-disassembly (Fig. 2g) followed by reassembly (analogous to Fig. 2a–f, omitted for brevity). These processes can be dynamically deployed to accommodate various operational demands. Collective transport allows the assembled shape to move together as a unified whole toward a specified target (Fig. 2i). Additional details of the self-reconfiguring algorithms are available in Methods and Supplementary Note 3.

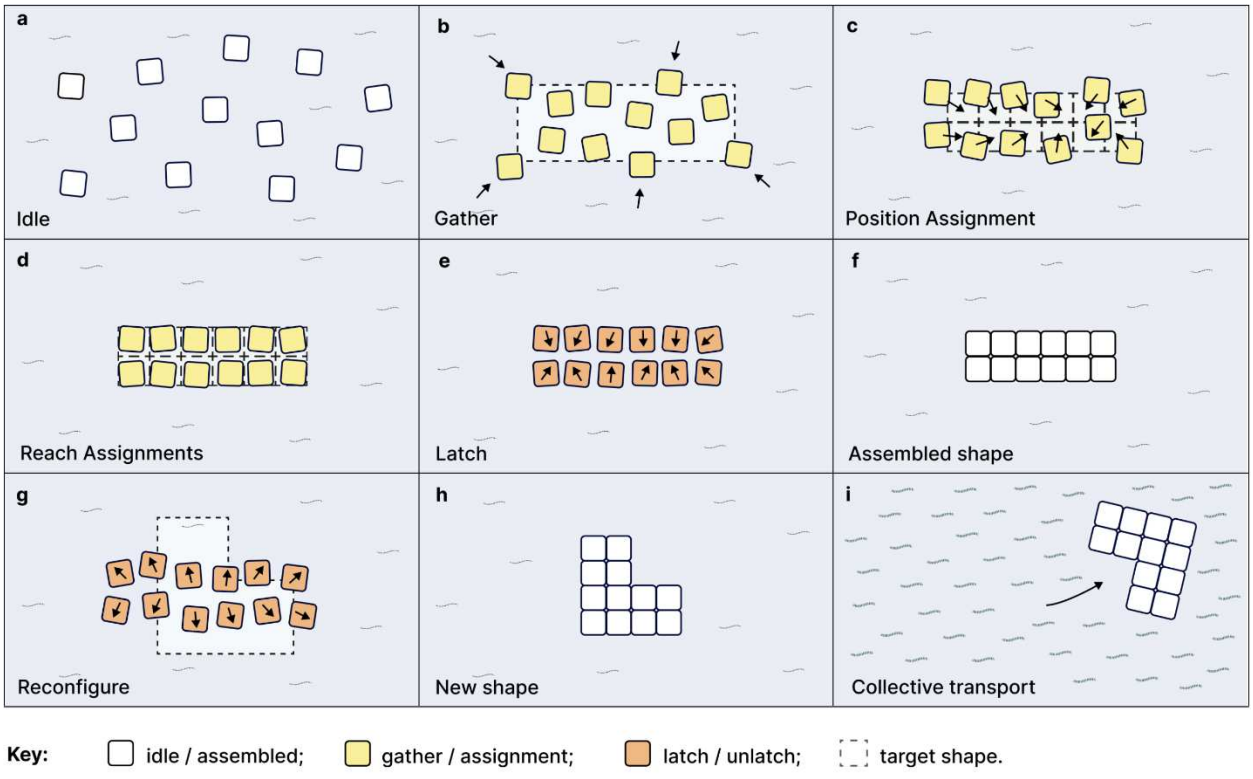

Fig. 2. Algorithmic steps towards self-assembly, self-reconfiguration, and collective transport in an

aquatic 2D MSRR system. (**a**) *FloatForm* modules remain idle or perform independent tasks while awaiting a shape command. (**b**) Upon receiving a new target shape, boats navigate toward the target configuration using a shape-reference formation algorithm. (**c**) Once in proximity of the desired shape, discrete positions are assigned via the Hungarian algorithm. (**d**) robots proceed to their designated positions using a position-reference formation algorithm. (**e**) Magnetic latching systems are activated to secure connections between neighboring units. (**f**) The structurally cohesive assembly. (**g**) A new shape command is received, the boats disassemble, repeating steps **a–f** to reconfigure into a new target configuration. (**h**) Completion of the reassembly process into the new shape. (**i**) The newly assembled structure moves collectively to a new destination.

Each *FloatForm* module operates with an identical code within the swarm. Initially, robots are randomly distributed across the water. Robots determine their positions and orientations using onboard sensors described earlier in this section (also see more details in Supplementary Note 1). To initiate self-assembly, a target shape $\boldsymbol{S}$, defined by a set of vertices, is transmitted to all robots within the swarm. The initial target shape is deliberately described as larger than the final desired configuration. The robots first gather and align within this preliminary shape using a distributed shape-reference formation algorithm based on potential field methods, incorporating attractive and repulsive forces. The attractive force guides the robots toward the target region, while the repulsive force mitigates collisions between robots (see more details in Methods). As most robots converge within the designated area, the shape progressively shrinks (Fig. 2b). This gradual reduction prevents congestion and enables the collective to transition smoothly into a configuration close to the final structure.

After completing the initial shape formation, minor misalignments may remain. To refine the structure, a centralized position assigner allocates new positions to the robots (Fig. 2c, Supplementary Note 3). Subsequently, a distributed position-reference formation algorithm guides the robots toward their designated positions within the defined shape (Fig. 2d, Supplementary Note 3). Once all robots have reached their

target locations, the magnetic latching mechanism engages, linking the robots into a rigid floating assembly (Fig. 2e, f). Following self-assembly, the collective may autonomously reconfigure in response to new shape commands issued by the task coordinator, or operate as a coherent robotic system capable of executing collective transport tasks. Upon activation of the self-reconfiguration process, the latching mechanisms disengage, and the robots move away from their attached neighbors by increasing repulsive forces in potential field methods (Fig. 2g). Once sufficiently dispersed, the robots reassemble into a new configuration using the same hybrid coordination strategy (Fig. 2h). We demonstrate collective transport following self-assembly (Fig. 2i). In this phase, each module is provided with center and orientation data of the goal shape, after which a position-reference potential field algorithm calculates the attractive forces that determine the reference velocity and heading needed to steer them to their assigned targets (see more details in Supplementary Note 3).

We validated this approach through experiments with four (Supplementary Video 3) and eight *FloatForm* modules (Fig. 3, Fig. 4, and Supplementary Video 4). As illustrated in Fig. 3, a group of eight robots successfully executed self-assembly, self-reconfiguration, and coordinated movement toward the corner of the tank. Each experiment required approximately 4–8 minutes. The corresponding trajectories of the robots are depicted in Fig. 4, clearly delineating each coordination phase. Across 10 experimental trials, the system achieved 90% and 70% success rates without human intervention in trials involving four and eight robots, respectively.

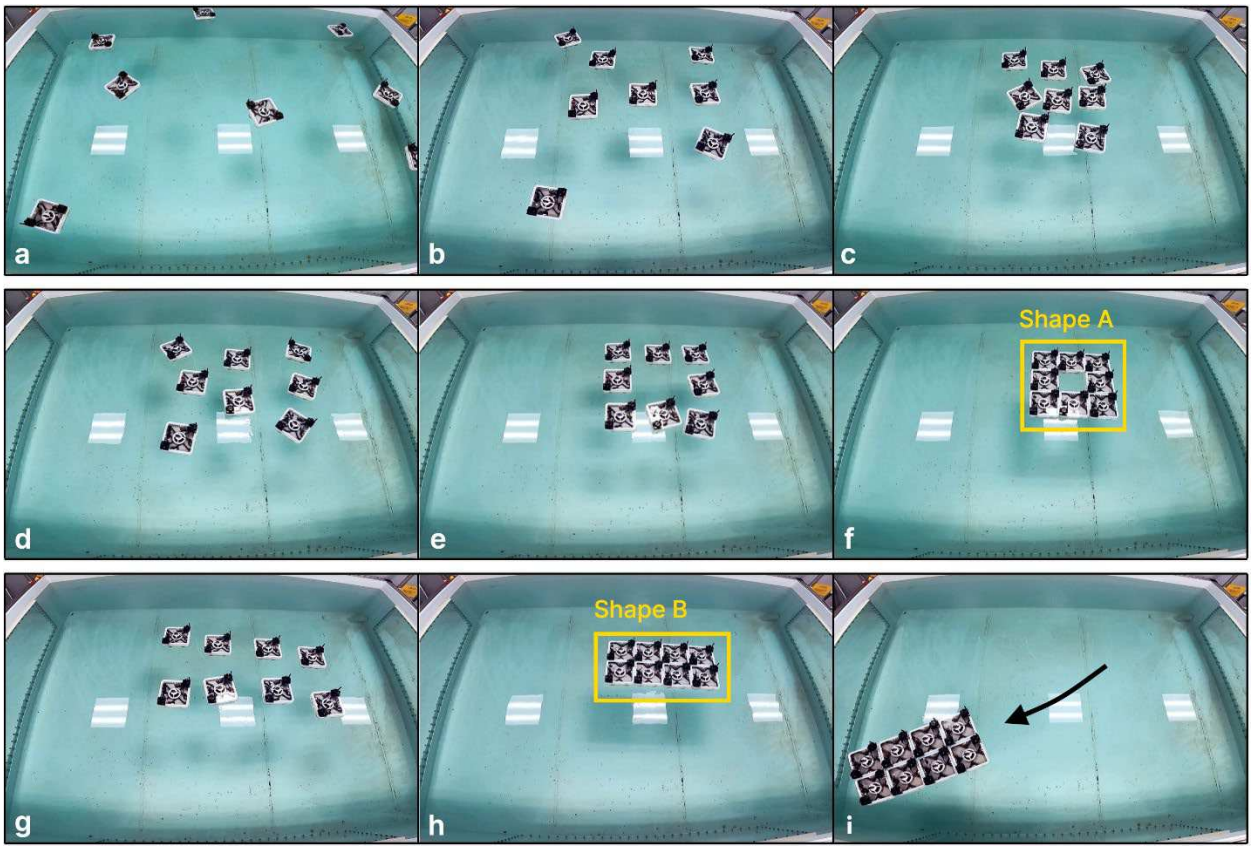

Fig. 3. Self-reconfiguration experiments with eight *FloatForm* modules. (**a**) Idle robots awaiting a target shape command. (**b**)-(**c**) The robots begin gathering within the approximate boundary of a target shape, "A". (**d**)-(**e**) Once the boats are within the boundary, discrete positions are assigned to each unit. (**f**) The boats then latch together to form a rigid structure. (**g**) A new target shape, "B", is received: the boats de-latch and the process repeats, as they reposition within the boundaries of shape "B", where discrete positions are reassigned, and the boats latch into the new configuration (**h**). (**i**) The newly formed structure maneuvers to the side of the pool.

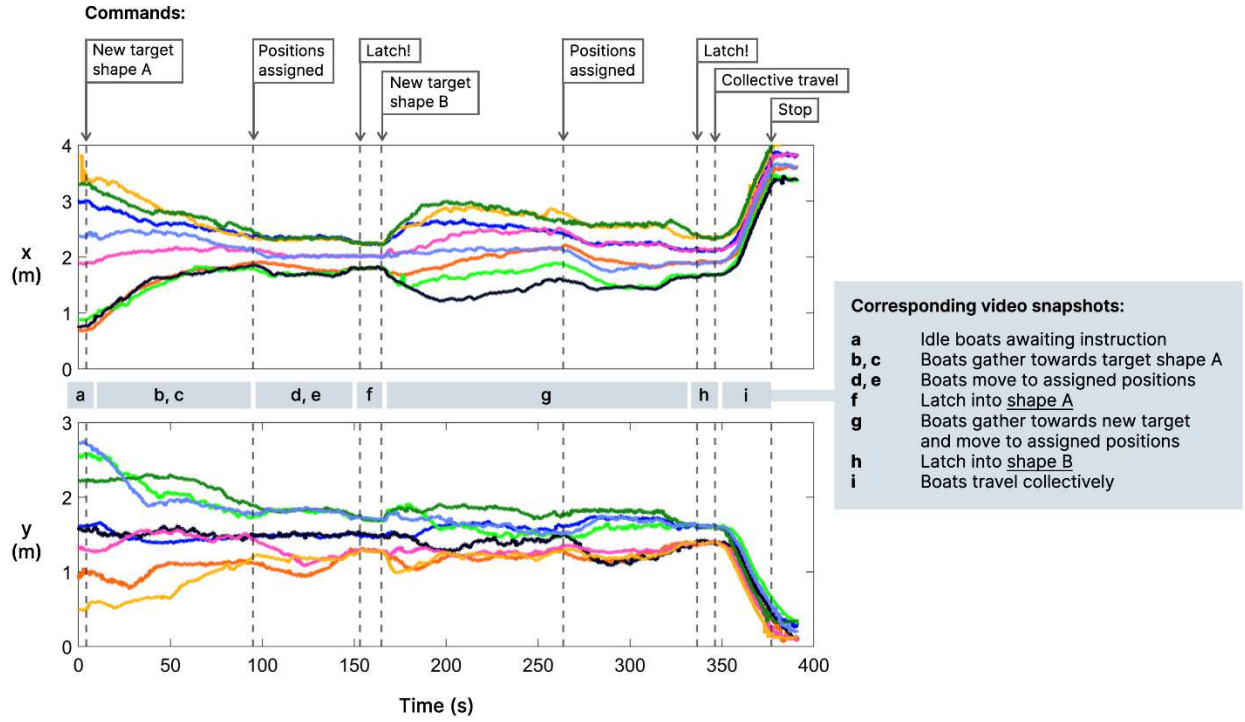

Fig. 4. *FloatForm* module trajectories during self-assembly and reconfiguration. The X and Y trajectories of eight *FloatForm* robots during the self-reconfiguration experiments shown in Fig. 3 and Supplementary Video 4, high-level commands to the boats are annotated at the top.

DISCUSSION

Self-reconfiguring aquatic robots opens new avenues from rapidly deployable floating structures (e.g., on-demand rafts and bridges) to scalable environmental monitoring and remediation tasks where adaptive spatial coverage is critical (e.g., in tracking algal blooms or responding to oil spills). Despite their potential, autonomous aquatic self-assembly and reconfiguration are challenged by complex, nonlinear hydrodynamics and persistent disturbances, demanding robust hardware and control platforms that support distributed autonomy and rapid, parallel coordination.

To address these challenges, we have introduced the *FloatForm* platform—a modular robotic system designed to perform parallel, largely decentralized self-assembly and self-reconfiguration on the water. *FloatForm* robots utilize a hybrid coordination framework as a strategy for robust robotic swarm behavior on the water. With each *FloatForm* module equipped with its own onboard sensing and computation, reliance on centralized control is minimized and individual robots can operate autonomously in response to higher-level commands. This decentralized approach means that the system can be scaled to larger formations without incurring significant communication overhead or computational complexity. Furthermore, the distributed nature of the control architecture enhances fault tolerance: in the event of an individual robot breaking down or losing communication, the swarm can dynamically reconfigure to maintain functionality. In aquatic environments, where disturbances and partial failures are common, the presence of a minimal high-level coordinator provides an effective means of correcting local imperfections and ensuring resilience.

Our successful indoor demonstrations, supported by a hybrid control architecture and reliable latching mechanism, establish a foundation for scaling up to real-world deployments. Looking ahead, we envision collective aquatic robotic systems performing tasks across a broad range of maritime applications, including forming temporary platforms for infrastructure inspection or maintenance. In oceanographic research, reconfigurable robot formations could enable adaptive sensor networks for studying migratory species or monitoring environmental changes. In offshore logistics and emergency response, modular robotic teams could function as reconfigurable docking stations or transport units for use in inaccessible areas. However, several practical challenges must be addressed before real-world deployments are viable. Current limitations include occasional failure modes such as collisions during latching or robots becoming trapped in local minima during shape formation. These deadlocks are presently resolved using stochastic perturbations, wherein robots 'shake' themselves free and retry latching. To enhance the reliability and efficiency of shape formation control, future efforts will replace the existing potential-field heuristic with an optimization-based control barrier function (CBF) approach[39]. This strategy is anticipated to provide stronger convergence guarantees and minimize error-prone behaviors during formation. Moreover, when *FloatForm*

is broadly dispersed to perform monitoring or search tasks, each module will require more advanced motion planning and control algorithms to ensure safe, robust navigation in realistic outdoor environments. We propose leveraging learning-based control techniques, such as data-driven Model Predictive Control (MPC)[40], which would allow robots to adapt in real time to changing conditions, obstacles, and noisy sensory inputs. Furthermore, we have demonstrated that, once assembled, the *FloatForm* swarm can execute coordinated movements as a single unit under calm conditions. However, maintaining stable collective motion in the presence of disturbances and minimal inter-robot communication remains an open challenge[31].

Additionally, open-water deployment will also require mechanical and sensing adaptation. Increasing the robot size could improve hydrodynamic stability and enable a broader range of tasks, which in turn calls for more robust latching systems capable of withstanding higher loads[41]. On the sensing side, replacing the current acoustic indoor localization system with outdoor-capable technologies such as GPS, vision-based tracking, or Doppler Velocity Logs will be essential. Robust onboard power and communication systems, potentially incorporating solar charging and distributed networking, will also be critical for sustained missions in remote environments.

FloatForm draws some inspiration from biological systems such as fire ants, which dynamically self-assemble into rafts and bridges to survive floods and cross gaps[35,36]. These natural swarms achieve robust collective behaviors through local rules and physical interactions, allowing the colony to adapt to complex, unpredictable environments without centralized control. Similarly, our system demonstrates that through minimal centralized coordination and largely distributed autonomy, robotic collectives can exhibit flexible self-assembly and self-reconfiguration in aquatic environments. This perspective underscores the promise of future aquatic swarm systems: resilient, reconfigurable, and capable of operating in the dynamic and uncertain conditions of the real world.

METHODS

FloatForm Module Design

The *FloatForm* hardware was designed with ease of fabrication and programming in mind, making it quick to assemble and conduct experiments involving larger numbers of robots. The hull, thrusters, and latching mechanisms are the core mechanical components. A square footprint was chosen, allowing boats to assemble into square lattices (Fig. 1). The manufacturing process consisted of resin-based 3D printing: hull and four thruster brackets, which hold the custom miniature thrusters (Fig. 1a), and laser-cutting of an acrylic top-plate. The thrusters, while compact, produce large forces (at low resolution) relative to the vehicle's overall inertia, resulting in aggressive rotational motions at near-zero speeds. To compensate, a basic set of fins were added along the x and y axes of the boats (Fig. 1c), increasing the hydrodynamic drag and facilitating less sensitive angular control at low speeds. Finally, a laser-cut acrylic cover protects the electronics from occasional water-splashes, while providing a supporting structure for the ultrasonic beacons and access points for battery charging via USB and a power switch. The current *FloatForm* design achieves 2D motion with a forward speed of 70 mm/s and near-zero turning radius around its center of mass.

To facilitate shape reconfiguration, each *FloatForm* robot must be capable of reliably latching and de-latching with other boats. The designed latching system is fully enclosed within the hull of the boat and makes use of an origami-inspired mechanism to simultaneously actuate permanent magnets on all four sides of the robot via a single lightweight servo motor located in the center of the robot (see Supplementary Fig. 1 and Supplementary Fig. 2a). The mechanism is based on a uniformly-scaling rotating polygon[42], with rotation at the center causing auxetic contraction of all four sides (Supplementary Fig. 2b). The auxetic mechanism is composed of rigid 3D printed elements (PLA 3D printed on a Prusa Mk3) with simple strips of synthetic rubber forming the compliant hinges. In the extended position (see Supplementary Fig. 2c), the magnets are in contact with the interior sides of the hull, allowing other boats in the working range (10 cm), to latch to the sides (see Supplementary Fig. 2e). When de-latching, the mechanism is rotated, pulling the

magnets inwards (see Supplementary Fig. 2b) and breaking attraction to neighboring robots (see Supplementary Fig. 2d). The auxetic mechanism is composed of rigid 3D printed elements (PLA 3D printed on a Prusa Mk3) with simple strips of rubber forming the compliant hinges. Magnets are arranged with alternating polarities, ensuring boats reliably latch into square lattice formations. The combined inertia of the mechanism and a 3D printed gearbox ensure that either latched or un-latched states can be maintained with no power to the motor (power is only required to change state).

More details of the mini thruster design, electronics and sensors and the robot localization can be found in Supplementary Note 1.

Low-level Feedback Control

The precise maneuvering of individual *FloatForm* modules in accordance with high-level planning objectives requires the implementation of feedback control. This approach enables the system to dynamically adapt to varying reference commands and sensor inputs, ensuring accurate steering adjustments for each robot. Here, we develop feedback controllers based on proportional–integral–derivative (PID) control to regulate each *FloatForm* robot's three degrees of freedom: surge, sway, and yaw. To account for nonlinear dynamics, we further employ feedback linearization. Additionally, given the constraints on the customized thruster's rotational speed and the over-actuated nature of the vehicle, a thrust allocation strategy is designed to distribute control commands optimally across the thrusters.

The surge and sway speed controller can receive reference velocities (u_d, v_d) from a user/operator or a higher-level algorithm. In this case, the references are provided by a higher-level algorithm for shape formation and reconfiguration. Considering that τ_u represents the force in the surge direction, and τ_v the force in the sway direction, velocity controllers can be designed following a PID-based approach as:

$$\tau_u = K_{pu} e_u + K_{iu} \int A e_u d\tau + K_{du} \dot{e}_u \quad (1)$$

$$\tau_v = K_{pv} e_v + K_{iv} \int e_v d\tau + K_{dv} \dot{e}_v \quad (2)$$

where $e_u = u_d - u, e_v = v_d - v$ are the velocity errors, u is the surge velocity, v is the sway velocity, and $K_{pu}, K_{iu}, K_{du}, K_{pv}, K_{iv}, K_{dv}$ are positive controller gains. With such controllers, the robots can follow time-varying reference velocities for any feasible task.

The heading control system is designed based on a cascade approach. First, the heading error is chosen as $e_\psi = \psi_d - \psi$, where ψ is the robot heading angle, and the desired heading ψ_d is a user-defined parameter, or dependent on the desired shape formation. Then, the high-level PID is designed as:

$$r_d = K_{p\psi} e_\psi + K_{i\psi} \int e_\psi d\tau + K_{d\psi} \dot{e}_\psi \quad (3)$$

where r_d is the desired yaw rate, and $K_{p\psi}, K_{i\psi}, K_{d\psi}$ are positive controller gains. Now, consider the following nonlinear model in yaw using Fossen's equations of motion for marine systems[43]:

$$\dot{r} = \frac{1}{I_z - N_{\dot{r}}} ((-X_{\dot{u}} + Y_{\dot{v}}) uv + N_r r + N_{r|r|} r|r| + \tau_r) \quad (4)$$

Here, r is the rotational speed, τ_r is the rotational moment, I_z is the moment of inertia, and $X_{\dot{u}}, Y_{\dot{v}}, N_r, N_{r|r|}, N_{\dot{r}}$ are hydrodynamic parameters. Then, the model can be rewritten as:

$$\dot{r} = f_r(r) + g_r(r) \tau_r \quad (5)$$

where $f_r(r)$ and $f_r(r)$ are defined as follows:

$$f_r(r) = \frac{(-X_{\dot{u}} + Y_{\dot{v}}) uv + N_r r + N_{r|r|} r|r|}{I_z - N_{\dot{r}}} \quad (6)$$

$$g_r(r) = \frac{1}{I_z - N_{\dot{r}}} \quad (7)$$

Next, applying a change of variable $\tau_r = u_r$, and feedback linearization, the low-level yaw controller can be designed based on a PD approach as:

$$u_r = \frac{1}{g_r(r)}(K_{pr}e_r + K_{dr}\dot{e}_r - f_r(r)) \quad (8)$$

with error $e_r = r_d - r$, and positive controller gains. Implementing feedback linearization allows us to compensate for nonlinear dynamics terms, which have a large effect on the yaw degree of freedom.

A detailed description of the thrust allocation is provided in Supplementary Note 2.

Hybrid Coordination Algorithm

The proposed hybrid coordination algorithm combines a lightweight centralized planner for high-level tasks—such as position assignment to refine shape formation—with distributed controllers onboard each robot to govern core behaviors, including shape formation and collision avoidance. We demonstrate three fundamental collective capabilities: (i) self-assembly, enabling the parallel formation of physically connected structures; (ii) self-reconfiguration, allowing the swarm to disassemble and reassemble into new physically connected configurations in parallel; and (iii) collective transport, enabling the assembled swarm to navigate cohesively across the water. As illustrated in Fig. 2, each collective capability consists of multiple sequential phases. For the gathering phase (Fig. 2b), a distributed shape-reference formation algorithm is implemented to drive the swarm gradually into the desired shape and a square lattice structure.

More specifically, the algorithm is based on the Artificial Potential Field method[44], which establishes so-called potential forces to control a system. Two main potential forces are considered in this work, an attractive force ($F_a \in R^2$) and a repulsive force ($F_r \in R^2$):

$$F_p = k_{p,1}F_a + k_{p,2}F_r \quad (9)$$

where $k_{p,1}, k_{p,2}$ are positive weighting parameters. Here, the attractive force is designed to drive the *Float-Form* robot to the desired region, whereas the repulsive force is applied to avoid collisions and create lattices between neighboring robots. First, let us consider the attractive force. The vehicle is given a desired shape, constructed by a matrix $V = [v_1, v_2, \ldots, v_W]^T$, composed by the shape vertices $v_w \in R^2$, where $w = 1,2, \ldots W$, and W is the total number of vertices. Next, a variable s is equal to 1 if a module is inside the shape, and -1 if the vehicle is outside the shape. Then, a distance vector d is evaluated with the robot position $p = [x, y]^T$ and its nearest vertex v_{nearest} as $d = v_{\text{nearest}} - p$. The attractive regional force is computed as

$$F_a = k_{a,1}\mathrm{s}\left(1 + \tanh\left(\frac{\mathrm{s}||d||}{k_{a,2}}\right)\right)\left(\frac{d}{||d||}\right) \tag{10}$$

where $k_{a,1}, k_{a,2}$ are positive parameters. Now, let us consider the repulsive force, which is composed of a collision element $F_c \in R^2$ and a lattice element $F_l \in R^2$, for each neighboring modules:

$$F_r = \sum_{n=1}^{N}\left(F_{c,n} + F_{l,n}\right) \tag{11}$$

with N as the total number of neighbors.

More specifically, for each neighboring module, $F_{c,n}$ and $F_{l,n}$ are computed with:

$$F_{c,n} = k_{r1}\left(\frac{r_0}{||r_n||} - \left(\frac{r_0}{||r_n||}\right)^2\right)\left(\frac{r_n}{||r_n||}\right) \tag{12}$$

$$F_{l,n} = \frac{-\sin(4\varphi_n)}{||r_n||}\left(\frac{r_n}{||r_n||}\right) \tag{13}$$

where $\varphi_n = \mathrm{atan2}(y_n - y, x_n - x)$ is the angle between the robot and the neighbor n, $r_n = p_n - p$ is the distance between the robot and the neighbor n, $p_n = [x_n, y_n]^T$ is the position of a neighboring module, and

$k_{r,1}, r_o$ are tuning parameters. Finally, since the potential field force F_p is computed in the inertial reference frame, it is rotated into the body frame with:

$$[u_d, v_d]^T = R(\psi)^T F_p \tag{14}$$

and its rotation matrix

$$R(\psi) = \begin{bmatrix} \cos\psi & -\sin\psi \\ \sin\psi & \cos\psi \end{bmatrix} \tag{15}$$

Finally, $[u_d, v_d]^T$ are saturated to user-defined maximum allowed velocities, and then sent as desired values to the robot's surge and sway speed controller.

Further details of the other phases of the algorithm such as the centralized task assignment and collective transport algorithm are provided in Supplementary Note 3.

References

1 Swissler, P. & Rubenstein, M. FireAntV3: A Modular Self-Reconfigurable Robot Toward Free-Form Self-Assembly Using Attach-Anywhere Continuous Docks. *IEEE Robotics and Automation Letters* **8**, 4911-4918 (2023).

2 Odem, S., Hacohen, S. & Medina, O. An RRT That Uses MSR-Equivalence for Solving the Self-Reconfiguration Task in Lattice Modular Robots. *IEEE Robotics and Automation Letters* **8**, 2922-2929 (2023).

3 Majed, A., Harb, H., Nasser, A. & Clement, B. RUN: a robust cluster-based planning for fast self-reconfigurable modular robotic systems. *Intelligent Service Robotics* **16**, 75-85 (2023).

4 Liu, C., Yu, S. & Yim, M. Motion Planning for Variable Topology Trusses: Reconfiguration and Locomotion. *IEEE Trans. Rob.* **39**, 2020-2039 (2023).

5 Dokuyucu, H. İ. & Özmen, N. G. Achievements and future directions in self-reconfigurable modular robotic systems. *Journal of Field Robotics* **40**, 701-746 (2023).

6 Nisser, M., Cheng, L., Makaram, Y., Suzuki, R. & Mueller, S. in *2022 International Conference on Robotics and Automation (ICRA)* 4254-4260 (2022).

7 Liang, G., Tu, Y., Zong, L., Chen, J. & Lam, T. L. in *2022 International Conference on Robotics and Automation (ICRA)* 4232-4238 (2022).

8 Tu, Y., Liang, G. & Lam, T. L. in *2021 IEEE International Conference on Robotics and Automation (ICRA)* 4252-4258 (2021).

9 Thalamy, P., Piranda, B. & Bourgeois, J. Engineering efficient and massively parallel 3D self-reconfiguration using sandboxing, scaffolding and coating. *Rob. Auton. Syst.* **146**, 103875 (2021).

10 Doyle, M. J. *et al.* Modular Fluidic Propulsion Robots. *Ieee Transactions on Robotics* **37**, 532-549 (2021). https://doi.org/10.1109/Tro.2020.3031880

11 Swissler, P. & Rubenstein, M. in *2020 IEEE/RSJ International Conference on Intelligent Robots and Systems (IROS)* 3340-3347 (2020).

12 Liang, G., Luo, H., Li, M., Qian, H. & Lam, T. L. in *2020 IEEE/RSJ International Conference on Intelligent Robots and Systems (IROS)* 6506-6513 (2020).

13 Swissler, P. & Rubenstein, M. in *2018 IEEE International Conference on Robotics and Automation (ICRA)* 6812-6817 (2018).

14 Suzuki, Y., Tsutsui, Y., Yaegashi, M. & Kobayashi, S. in *2017 IEEE International Conference on Robotics and Automation (ICRA).* 2131-2137.

15 Klidbary, S. H., Shouraki, S. B. & Kourabbaslou, S. S. Path planning of modular robots on various terrains using Q-learning versus optimization algorithms. *Intelligent Service Robotics* **10**, 121-136 (2017). https://doi.org/10.1007/s11370-017-0217-x

16 Gilpin, K. & Rus, D. Modular Robot Systems. *IEEE Robotics & Automation Magazine* **17**, 38-55 (2010).

17 An, B. K. EM-Cube: Cube-shaped, self-reconfigurable robots sliding on structure surfaces. *Ieee Int Conf Robot*, 3149-3155 (2008).

18 Daudelin, J. *et al.* An integrated system for perception-driven autonomy with modular robots. *Sci Robot* **3** (2018). https://doi.org/ARTN eaat498310.1126/scirobotics.aat4983

19 Yim, M. *et al.* Modular self-reconfigurable robot systems - Challenges and opportunities for the future. *Ieee Robot Autom Mag* **14**, 43-52 (2007). https://doi.org/Doi 10.1109/Mra.2007.339623

20 Rubenstein, M., Cornejo, A. & Nagpal, R. Programmable self-assembly in a thousand-robot swarm. *Science* **345**, 795-799 (2014). https://doi.org/10.1126/science.1254295

21 Khodr, H., Mutlu, M., Hauser, S., Bernardino, A. & Ijspeert, A. An Optimal Planning Framework to Deploy Self-Reconfigurable Modular Robots. *Ieee Robotics and Automation Letters* **4**, 4278-4285 (2019). https://doi.org/10.1109/Lra.2019.2931216

22 Mutlu, M., Hauser, S., Bernardino, A. & Ijspeert, A. Playdough to Roombots: Towards a Novel Tangible User Interface for Self-reconfigurable Modular Robots. *2018 Ieee International Conference on Robotics and Automation (Icra)*, 1970-1977 (2018).

23 Hauser, S. *et al.* Roombots extended: Challenges in the next generation of self-reconfigurable modular robots and their application in adaptive and assistive furniture. *Robot Auton Syst* **127** (2020). https://doi.org/ARTN 10346710.1016/j.robot.2020.103467

24 Romanishin, J. W., Gilpin, K., Claici, S. & Rus, D. 3D M-Blocks: Self-reconfiguring Robots Capable of Locomotion via Pivoting in Three Dimensions. *2015 Ieee International Conference on Robotics and Automation (Icra)*, 1925-1932 (2015).

25 Romanishin, J. W., Mamish, J. & Rus, D. Decentralized Control for 3D M-Blocks for Path Following, Line Formation, and Light Gradient Aggregation. *Ieee Int C Int Robot*, 4862-4868 (2019). https://doi.org/10.1109/iros40897.2019.8967810

26 Oung, R. & D'Andrea, R. The Distributed Flight Array: Design, implementation, and analysis of a modular vertical take-off and landing vehicle. *Int J Robot Res* **33**, 375-400 (2014). https://doi.org/10.1177/0278364913501212

27 Saldaña, D., Gabrich, B., Li, G. R., Yim, M. & Kumar, V. ModQuad: The Flying Modular Structure that Self-Assembles in Midair. *2018 Ieee International Conference on Robotics and Automation (Icra)*, 691-698 (2018).

28 Baldassarre, G. *et al.* Self-organized coordinated motion in groups of physically connected robots. *Ieee T Syst Man Cy B* **37**, 224-239 (2007). https://doi.org/10.1109/Tsmcb.2006.881299

29 Tu, Y. X., Liang, G. Q. & Lam, T. L. FreeSN: A Freeform Strut-node Structured Modular Self-reconfigurable Robot - Design and Implementation. *2022 Ieee International Conference on Robotics and Automation (Icra 2022)*, 4239-4245 (2022). https://doi.org/10.1109/Icra46639.2022.9811583

30 Du, Z., Negenborn, R. R. & Reppa, V. Review of floating object manipulation by autonomous multi-vessel systems. *Annu Rev Control* **55**, 255-278 (2023). https://doi.org/10.1016/j.arcontrol.2022.10.003

31 Wang, W. *et al.* Distributed Motion Control for Multiple Connected Surface Vessels. *2020 Ieee/Rsj International Conference on Intelligent Robots and Systems (Iros)*, 11658-11665 (2020). https://doi.org/10.1109/Iros45743.2020.9340743

32 Paulos, J. *et al.* Automated Self-Assembly of Large Maritime Structures by a Team of Robotic Boats. *Ieee T Autom Sci Eng* **12**, 958-968 (2015). https://doi.org/10.1109/Tase.2015.2416678

33 O'Hara, I. *et al.* Self-Assembly of a Swarm of Autonomous Boats into Floating Structures. *2014 Ieee International Conference on Robotics and Automation (Icra)*, 1234-1240 (2014).

34 Furno, L., Blanke, M., Galeazzi, R. & Christensen, D. J. Self-reconfiguration of Modular Underwater Robots using an Energy Heuristic. *2017 Ieee/Rsj International Conference on Intelligent Robots and Systems (Iros)*, 6277-6284 (2017).

35 Mlot, N. J., Tovey, C. A. & Hu, D. L. Fire ants self-assemble into waterproof rafts to survive floods. *P Natl Acad Sci USA* **108**, 7669-7673 (2011). https://doi.org/10.1073/pnas.1016658108

36 Wagner, R. J., Lamont, S. C., White, Z. T. & Vernerey, F. J. Catch bond kinetics are instrumental to cohesion of fire ant rafts under load. *P Natl Acad Sci USA* **121** (2024). https://doi.org/ARTN e231477212110.1073/pnas.2314772121

37 Gheneti, B. *et al.* Trajectory Planning for the Shapeshifting of Autonomous Surface Vessels. *2019 International Symposium on Multi-Robot and Multi-Agent Systems (Mrs 2019)*, 76-82 (2019). https://doi.org/10.1109/mrs.2019.8901099

38 Knizhnik, G. & Yim, M. Amplitude Control for Parallel Lattices of Docked Modboats. *2022 Ieee International Conference on Robotics and Automation (Icra 2022)*, 3027-3033 (2022). https://doi.org/10.1109/Icra46639.2022.9812381

39 Xiao, W., Belta, C. A. & Cassandras, C. G. High Order Control Lyapunov-Barrier Functions for Temporal Logic Specifications. *P Amer Contr Conf*, 4886-4891 (2021).

40 Rosolia, U., Zhang, X. J. & Borrelli, F. Data-Driven Predictive Control for Autonomous Systems. *Annu Rev Contr Robot* **1**, 259-286 (2018). https://doi.org/10.1146/annurev-control-060117-105215

41 Fernández-Gutiérrez, D. *et al.* Design of an Autonomous Latching System for Surface Vessels. *2022 Ieee International Conference on Robotics and Automation (Icra 2022)* (2022). https://doi.org/10.1109/Icra46639.2022.9811754

42 Ou, J. F. *et al.* KinetiX - designing auxetic-inspired deformable material structures. *Comput Graph-Uk* **75**, 72-81 (2018). https://doi.org/10.1016/j.cag.2018.06.003

43 Thor, I. F. *Handbook of Marine Craft Hydrodynamics and Motion Control*. (Wiley, 2021).

44 Hou, S. P. & Cheah, C. C. Dynamic compound shape control of robot swarm. *Iet Control Theory A* **6**, 454-460 (2012). https://doi.org/10.1049/iet-cta.2011.0115

Data Availability All data to support the findings of this study are available from the corresponding authors upon request.

Code Availability All the data analyses were performed using custom scripts written in MATLAB 2024b. All codes to support the findings of this study are available from the corresponding authors upon request.

Acknowledgements We thank Jingxian Wang and David Fernandez-Gutierrez for their early discussions and implementation of the shape formation algorithm, and Yuki Machida for help with the electronics. We would like to thank Michael Triantafyllou for providing the small tank at Sea Grant, which was crucial for

conducting our experiments. We also extend our thanks to Fábio Duarte for his early discussions and coordination of this project.

Funding This research was supported by a grant from the Amsterdam Institute for Advanced Metropolitan Solutions (AMS) in the Netherlands.

Author Contributions W.W., N.H., C.R. and D.R. proposed the research and conceptual design of the *FloatForm* system. W.W. and N.H. designed hardware (hull design, latching mechanism, custom thrusters) and electronics. W.W. and A.G. developed robot control and software. W.W., A.G., N.H., and D.R. conducted the experiments. All authors analyzed and visualized data and contributed to the writing of the paper.

Correspondence Correspondence and requests for materials should be addressed to W.W. (email: wwang745@wisc.edu, and D.R. (email: rus@csail.mit.edu).

Competing Interests The authors declare that they have no competing interests.

Supplementary Files

This is a list of supplementary files associated with this preprint. Click to download.

- FloatFormSI.pdf
- S1.mp4
- S2.mp4
- S3.mp4
- S4.mp4